European Conference on Computational Fluid Dynamics
ECCOMAS CFD 2006
P. Wesseling, E. Oñate and J. Périaux (Eds)

YEE'S SCHEME FOR THE INTEGRATION OF MAXWELL'S EQUATION ON UNSTRUCTURED MESHES

Igor Sazonov*, Oubay Hassan*, Ken Morgan*, Nigel P. Weatherill*

*Civil & Computational Engineering Centre,
University of Wales Swansea
Singleton Park, Swansea, SA2 8PP, U.K.
e-mail: i.sazonov@swansea.ac.uk

Key words: Co-volume method, Yee's scheme, Delaunay triangulation, Voronoi tessellation

Abstract. *The co-volume integration method, Yee's scheme, generalized to unstructured mesh is considered and compared with time domain finite element method (TDFE). In order to generate the meshes for which a good quality dual mesh is ensured, a new point placing method for the generation of meshes appropriate for the use of the co-volume method is proposed. Numerical examples are presented which demonstrate the consistency and performance of the co-volume method.*

1 INTRODUCTION

Yee's scheme [1] is an example of co-volume method for the integration of Maxwell's equations. As it is staggered both in space and time, the Yee algorithm is a very fast and accurate method compared, for example, with the time domain finite element method (TDFE). Being based on the integral form of the Maxwell's equation, Yee's scheme preserves energy, and hence, maintain the amplitude of the plane waves. In addition, compared to nodal Finite Elements methods, the Yee algorithm is able to accurately approximated the electromagnetic field near boundary peculiarities such as sharp corner, vertex and wire structure. Therefore, there is no necessity to reduce the size of the elements in the vicinity of such peculiarities which will result in a big increase in the computation time.

Initially proposed for structured grids, the Yee's scheme can be generalized for unstructured meshes and that will enable its application to industrially complex geometries [2]. However, despite the fact that real progress has been achieved in unstructured mesh generation methods over the last two decades, Yee's scheme has not widely been used for problems which involve complex geometries. This is due to the difficulties encountered when attempting to generate high quality meshes, satisfying the requirements necessary for this method.

Yee's scheme requires two orthogonal meshes for the electric and magnetic fields. The dual Delaunay-Voronoi diagram is an obvious choice. In three-dimensional case, every edge of Voronoï diagram is orthogonal to the correspondent face of Delaunay triangulation, and vice verse. Since the time step limitation of Yee's algorithm is proportional to the shortest edge of both dual meshes, it is critical that the Voronoi diagram is as regular as the Delaunay triangulation.

In this work the co-volume method for fully unstructured tetrahedra mesh has been implemented and applied to the computation of the scattering of electromagnetic wave by perfectly conducting objects. Initially, bodies which can be fitted into 3D ideal mesh are considered. However, a new point placing method is proposed which enables meshes appropriate for the use with the co-volume method to be build. Using the mesh generated by this approach, the scattering of electromagnetic wave by a perfectly conducting sphere is computed by the co-volume method.

2 YEE'S Algorithm for Unstructured Grid

The Yee algorithm is based on two integral equations: Ampere's law

$$\frac{\partial}{\partial t}\int_A \boldsymbol{E}\, d\boldsymbol{A} = \varepsilon \oint_{\partial A} \boldsymbol{H}\, d\boldsymbol{l} \tag{1}$$

and Faraday's law

$$\frac{\partial}{\partial t}\int_A \boldsymbol{H}\, d\boldsymbol{A} = -\mu \oint_{\partial A} \boldsymbol{E}\, d\boldsymbol{l} \tag{2}$$

applied to a surface A and its boundary ∂A. Here $d\boldsymbol{A}$ is element of the surface area directed to the normal to the surface, $d\boldsymbol{l}$ is element of the contour length directed to the tangent to the contour.

The domain of interest is discretized using a dual Delaunay-Voronoi diagram. The Delaunay-Voronoi dual diagram contains Delaunay edges connecting two neighbour nodes, and Voronoi edges connecting circumcentra of two adjusted tetrahedron elements.

Consider ith Delaunay edge and orthogonal to it ith Voronoi face, figure 1*a*. Let l_i^D and A_i^V be the edge's length and the face's area, respectively. Denote by $\mathscr{V}_i = \{j_{i,1}, \ldots, j_{i,M_i^V}\}$ the set of Voronoi edges forming the boundary of Voronoi face correspondent to the ith Voronoi edge. Let E_i be the projection of the electric field onto the ith Delaunay edge in the point of intersection of the edge and the Voronoi face.

Now consider jth Voronoi edge and orthogonal to it jth Delaunay face, figure 1*b*. Let l_i^V and A_i^D be the edge's length and the face's area, respectively. Denote by $\mathscr{D}_j = \{i_{j,1}, \ldots, i_{j,M_i^D}\}$ the set of Delaunay edges forming the boundary of jth Delaunay face. Let H_j be the projection of magnetic field in the point of crossing the jth Voronoi edge and the jth Delaunay face.

If edges of the both meshes are directed, then the sign of the field projection onto the edge is unique.

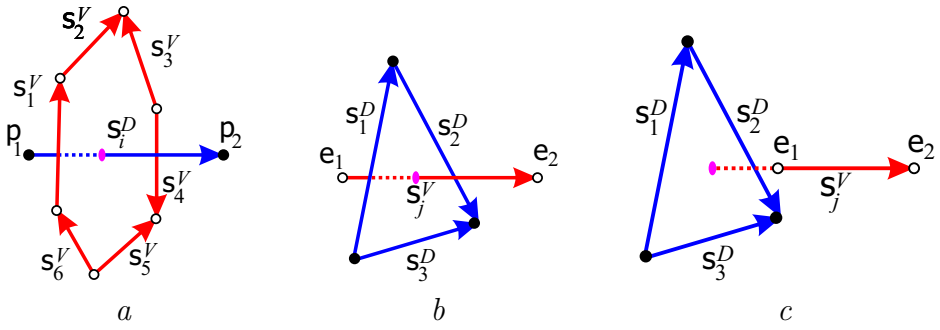

Figure 1: Delaunay edge s_i^D connecting nodes p_1-p_2 and correspondent Voronoi face formed by Voronoi edges $s_1^V, \ldots, s_6^V$ (a). Voronoi edge s_j^V connecting circumcentra of elements e_1-e_2 and correspondent Delaunay face formed by Delaunay edges $s_1^D, \ldots, s_3^D$ $(b$-$c)$. In (c) the Voronoi edge does not intersect the correspondent Delaunay face.

Using the above assumption, the following approximation of the Ampere and Faraday laws can be written.

$$\frac{\partial E_i}{\partial t} A_i^V = \varepsilon \sum_{k=1}^{M_i^V} H_{j_{i,k}} \, l_{j_{i,k}}^V \tag{3}$$

$$\frac{\partial H_j}{\partial t} A_j^D = -\mu \sum_{k=1}^{M_j^D} E_{i_{j,k}} \, l_{i_{j,k}}^D. \tag{4}$$

A staggered scheme is employed to integrate the above equations in time. Here the electric field is evaluated at $t = n\Delta t$ and the magnetic field is calculated at $t = (n+0.5)\,\Delta t$

$$E_i^n = E_i|_{t=n\Delta t}\,, \qquad H_j^{n+0.5} = H_j|_{t=(n+0.5)\Delta t} \tag{5}$$

A central differences approximation of the derivative is employed

$$\left(\frac{\partial E_i}{\partial t}\right)^{n+0.5} \approx \frac{E_i^{n+1} - E_i^n}{\Delta t} \qquad \left(\frac{\partial H_j}{\partial t}\right)^{n} \approx \frac{H_j^{n+0.5} - H_j^{n-0.5}}{\Delta t} \tag{6}$$

Substituting (6) into (3) and (4) we obtain the equations of an explicit staggered scheme

$$H_j^{n+0.5} = H_j^{n-0.5} - \frac{\mu \Delta t}{A_j^D} \sum_{k=1}^{M_j^D} E_{i_{j,k}}^n \, l_{i_{j,k}}^D \tag{7}$$

$$E_i^{n+1} = E_i^n + \frac{\varepsilon \Delta t}{A_i^V} \sum_{k=1}^{M_i^V} H_{j_{i,k}}^{n+0.5} \, l_{j_{i,k}}^V \tag{8}$$

In these equations as well as in subsequent formulas, indexes i and j are $i = 1, \ldots, N_s^D$; $j = 1, \ldots, N_s^V$ where N_s^D and N_s^V are numbers of Delaunay and Voronoi sides in the mesh.

Due to the symmetry of Maxwell's equations with respect to magnetic and electric field, it is possible to deal with electric field on Voronoi edges, E_j, and magnetic field on Delaunay edges, H_i. However, since the electric field on the boundary is required to impose the appropriate condition for perfect conductor, it is more suitable to deal with electric field on Delaunay edges.

Since the resultant scheme is explicit, a limitation on the size of the time step is required to ensure the stability of the scheme. For a structured grid, the stability criterium is derived in [6] and given by $c\Delta t < l/\sqrt{3}$ where $c = 1/\sqrt{\varepsilon\mu}$ is the light speed, and l is the edge length. For an unstructured tetrahedral mesh, there is no such simple criteria but computations show that we can use the following relation with a safety factor S_f

$$c\Delta t < S_f \min_{i,j}\{l_i^V, l_j^D\} \tag{9}$$

The implementation of the co-volume algorithm reuires the following arrays associated with the edges to be stored: Delaunay edge lengths, l_i^D; Voronoi face areas, A_i^V; projection of electric field, E_i; Voronoi edge lengths, l_j^V; Delaunay face areas, A_j^D; projection of magnetic field, H_j. An array of $3 * N_s^V$ is also required to store the connectivities between both types of edges, $i_{j,k},\ k = 1, 2, 3$. In this array, the number of the three edges surrounding each Voronoi side are stored. The edge number can be positive or negative dependent on the mutual orientation of jth Voronoi side and the $i_{j,k}$th Delaunay edge. We define the mutual orientation of side $p_1{-}p_2$ and $e_1{-}e_2$ as positive if the volume of the tetrahedron $p_1{-}p_2{-}e_1{-}e_2$ is positive. For example, in figure $1b$, side s_1^D is oriented negatively with respect to s_j^V whereas side s_3^D is oriented positively.

If the mesh contain N_p nodes and N_e tetrahedron elements, then the following approximate relations are valid for a typical mesh

$$\begin{array}{rcl} N_e & \approx & 6\,N_p \\ N_s^D & \approx & 7\,N_p \\ N_s^V & \approx & 2\,N_e \ \approx \ 12\,N_p \end{array} \tag{10}$$

From these it can be shown that approximately 19 unknowns fall at every node: 7 projections of electric field and 12 projections of magnetic field. For comparison, in the FE method 6 unknowns fall at every node: 3 components of electric field and 3 components of magnetic field. These means that for the same tetrahedral mesh the number of unknowns is approximately three times higher in the co-volume scheme than in FE method. Hence, we can expect that a coarser mesh can be used to obtain the same resolution of magnetic field. An increase in the mesh spacing by a factor of $(19/3)^{1/3} \approx 1.5$ can be used to generate the coarser meshes which maintain the same accuracy of the FE method, ie. instead of 15 points per wavelength it is sufficient to use 10 points per wavelength. In three dimension, this will results in three times smaller meshes than that required for the traditional node based FE method. However, it has to be mentioned that, for the same mesh, the storage required for the co-volume method is twice that required by the FE method.

3 Mesh Generation for Co-volume Method

3.1 Mesh Requirements

Formula (9) indicates that the important criterium for the mesh to be used efficiently with the co-volume method, is the absence of very short edges, in order to prevent the need to reduce the size of the time step which in turn conceals all advantages of the co-volume scheme.

Another important criterium is the absence of 'bad' elements. We consider the tetrahedron element as a bad, if its circumcentre is located outside the element. In this case the Voronoi edge will not intersect the Delaunay face, and the contour integral $\int_l \boldsymbol{H}\, d\boldsymbol{l}$ in (1) will be approximated by a value of magnetic field outside the correspondent Voronoi edge (figure 1c). This approximation of the integral cannot guarantee even the first order accuracy.

Here we define two quantitative criteria

$$r_{\text{bad}} = \frac{N_e^{\text{bad}}}{N_e} \tag{11}$$

$$Q = \frac{\min\limits_{i,j}\{l_i^D, l_j^V\}}{\langle l_i^D \rangle} \tag{12}$$

While generating the mesh, r_{bad} must be minimized and Q must be maximised.

The following element quality measure is used to classify the generated elements

$$q_e = 3\,\frac{d_e}{R_e} \tag{13}$$

where R_e is its circumradius, $d_e = \min\limits_{k=1,4} d_{e,k}$ is the signed distance from the circumcentre to the corresponding element faces. The signed distance means that it is negative if the circumcentre lies outside the element. Hence $q_e < 0$ indicates that the element e is bad, while $q_e = 1$ indicate a perfect tetrahedron.

It can be shown that if $q_e > 0$ for all elements, the mesh is guaranteed to be Delaunay.

It can also be shown that an element can have $q_e > 0$ only if all its faces are acute triangles. From here follows that a 3D mesh without bad elements can only be built provided *all boundary triangles are acute*.

Classical Yee's scheme on structured grid is second order accurate [3]. This is due to the fact that the surface integrals in (1)–(2) are approximated by the value taken just in face's barycentre, and the contour integrals are approximated by value taken in just edge's midpoints. For unstructured tetrahedral meshes, Voronoi (Delaunay) faces and Delaunay (Voronoi) edges are not guaranteed to intersected at face's barycentre and edge's midpoint. Hence, the generalization of the three dimensional Yee's scheme to unstructured grid will results in a reduction in the order of accuracy. Therefore, further criteria which limit the deviation of edge/face intersection point from the edge's mid-point and the face's barycentre can be included.

3.2 Traditional meshing methods

Traditional unstructured mesh generation methods, such as the advancing front technique (AFT) [2] and the Delaunay triangulation [9], are not designed to guarantee the creation of a mesh meeting the above requirements. These methods generate meshes in which the element edge length is acceptable, but, the corresponding Voronoï diagram is often highly irregular, with some very short Voronoï edges. Hence, they do not guarantee the regularity of the edge lengths of the dual mesh and the absence of bad elements.

One of promising approaches is the construction of the centroidal Voronoï tessellation and its dual Delaunay mesh. A Voronoï tesselation (VT) is called centroidal (CVT) if nodes of the dual Delaunay mesh coincide with the barycentra (mass centroids) of the corresponding Voronoï cells [10]. Although the quality of the final mesh is much higher than a mesh built by other methods, it is still not enough for the successful application of co-volume integration schemes.

3.3 Stitching method

An alternative approach is the stitching method developed for 2D meshes [8]. In this approach, the problem of triangulation is split into a set of relatively simple problems of local triangulation. Firstly, in the vicinity of boundaries, body fitted local meshes are built with properties close to those regarded as being ideal. An ideal mesh is employed, away from boundaries, to fill the remaining part of the domain. The two meshes are then combined, to form a consistent mesh, with the outer layer of the near boundary elements stitched to a region of ideal mesh by a special procedure. As a result, the quality of meshes built by the stitching method is higher when compared to those built by other known methods [8].

To generalize this method into 3D, several problems must be solved. The first issue is to build the ideal 3D mesh and the near-boundary triangulation.

3.3.1 Ideal mesh

A 3D analogue of this ideal mesh consists of equal non–perfect tetrahedra, each face of which is an isosceles triangle with one side of length l^D_{long} and two shorter sides of length $l^D_{\text{short}} = (\sqrt{3}/2)\, l^D_{\text{long}}$. Six such tetrahedra form a parallelepiped tiling the space, as illustrated in figure 2 [7]. It can be shown that this configuration maximises the minimal Voronoï edge for a fixed element size. All Voronoï edges have the same length $l^V \approx 0.35\, l^D_{\text{long}}$.

In this mesh $r_{\text{bad}} = 0$ and $Q = 0.38$ and $q_e \approx 0.95$ for all e.

3.3.2 Nearly boundary triangulation

If the domain boundary is smooth enough (i.e. if its curvature radius is much greater than element size) then building the first few layers is an elementary task in 2D case:

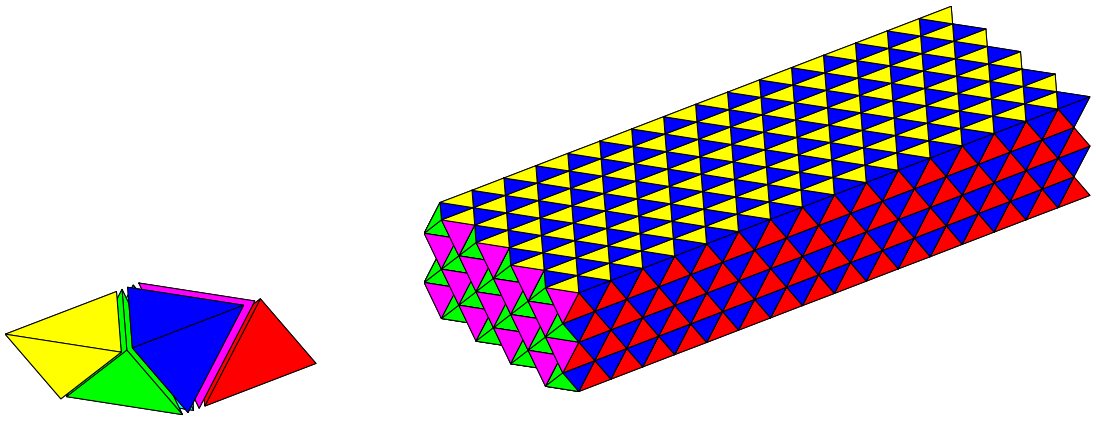

Figure 2: Six tetrahedra forming parallelepiped tiling the space (left). Waveguide made of such tetrahedra (right).

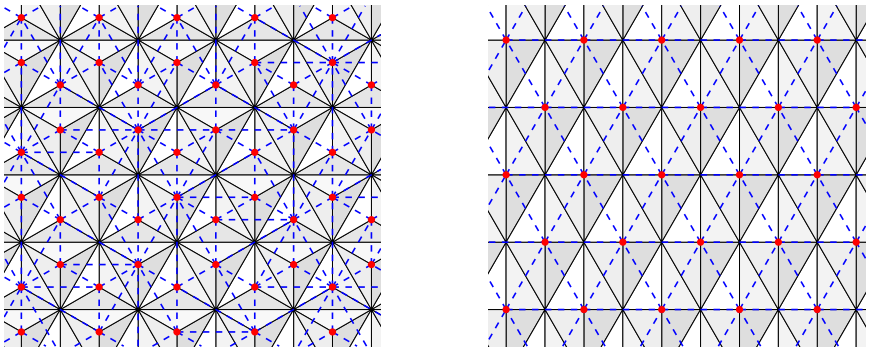

Figure 3: New tetrahedra (grey), their apexes (red) and Delaunay connection of the apexes (blue). Apex above the triangle centre (left) and above its edge (left). View from above the boundary.

the near-boundary mesh has the same topology as the 2D ideal mesh. A well tuned 2D advancing front method produces this near-boundary high-quality mesh [8].

The analogous 3D problem is much more complicated even for a simple, plane boundary with a 2D ideal boundary triangulation. Following the 3D advancing front technique, which is regarded to be a good method for placing points, we build a perfect tetrahedron on every boundary triangle (figure 3). It can be seen that the first layer of new points, i.e. tetrahedra apexes, form a hexagonal structure, similar to Voronoï vertices of the 2D ideal mesh, and cannot be connected to form all acute triangles. Therefore the standard advancing front method can not be applied directly to produce the required mesh quality.

Analyzing the structure of the 3D ideal mesh we can conclude that the best placing of a new point is above the edge shared by two conjugate surface triangles. To reproduce

the topology of the 3D ideal mesh using the advancing front method, we split the set of all boundary faces by non-intersecting pairs of triangles sharing the same edge. Then we locate a new point (tetrahedron's apex) above this edge (figure 3). In the case of ideal boundary triangulation, the optimal position of the apex is 0.684 of the boundary edge length. This procedure guarantees that the quality of the worst element reaches its maximum $q_e = 0.795$.

In the case of general boundary triangulation, we cannot split the set of boundary triangles into a non-intersecting pairs. In the case of an isolated single triangle, the new point is located above its circumcentre in a similar manner to the standard advancing front method. In our present method, we do not follow the traditional advancing front method by creating points and elements simultanuously. Elements are only created layer by layer starting from the boundary triangulation. After all the points on the next layer are created using the above technique, the Delaunay method is used to create the new set of tetrahedral elements. This method can be viewed as a sophisticated version of 3D advancing front method (for placing points) coupled with the Delaunay method (for connecting points).

In order to evaluate the quality of the elements generated using the proposed method, a simple domain, made of two spherical surfaces, is considered. A cut through the triangulation is shown in Figure 4. The mesh contains some bad elements but they share is $r_{\text{bad}} = 0.12\%$ only. The shortest Voronoï edge is $Q = 0.05$ of average Delaunay edge length. The domain is also triangulated using the standard advancing front method, the

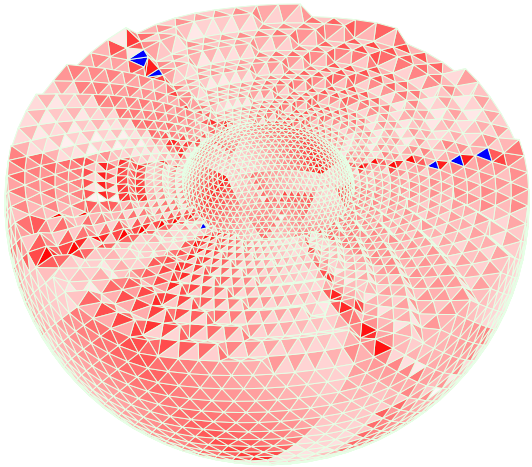

Figure 4: Cut of the triangulation of a spherical layer by the proposed method. Bad elements are indicated by blue. Intensity of red indicates the quality of not-bad elements: the better is the element, the whiter is its color.

Delaunay method and the CVT method. Table one show a comparison between various

Table 1: Comparison of different meshing methods

Mesh quality creteria		Mesh generation method			
		AFT	Delaunay	CVT	Proposed
Q		$4 \cdot 10^{-7}$	$2.4 \cdot 10^{-6}$	$1.0 \cdot 10^{-5}$	$4.8 \cdot 10^{-2}$
r_{bad}		67%	50%	9.8%	0.12%
q_e	min	-3	-2.2	-1.2	-0.02
	mean	-0.49	-0.07	0.39	0.65
$\frac{3R_e^{\text{in}}}{R_e}$	min	$3{\cdot}10^{-4}$	$5{\cdot}10^{-3}$	0.08	0.74
	mean	0.65	0.72	0.88	0.92
$\frac{3}{\kappa}$, [11]	min	0.03	0.06	0.15	0.93
	mean	0.89	0.91	0.97	0.984
$\min \frac{h_e^{\min}}{l_e^{\max}}$		$1.5{\cdot}10^{-3}$	$3.0{\cdot}10^{-3}$	$4.6{\cdot}10^{-3}$	0.42

mesh quality criteria evaluated on the four generated meshes.

In addition to the criteria described earlier, some standard element quality measures are also evaluated: the ratio of inradius to the circumradius, $3R^{\text{in}}/R_e$, algebraic metric, $3/\kappa$, introduced in [11] (factor 3 in the both cases provides the value one for the perfect tetrahedron) and the ratio of the minimal tetrahedron height to its longest edge, $h^{\min}/l^D_{\max}$, which is a very important measure as it relates to the stability requirement of the traditional finite element method.

From Table 1, it is clear that a superior element quality, measured by any criterion, is obtained using the newly proposed technique.

4 NUMERICAL EXAMPLES

4.1 Waveguide

The first example consider the propagation of electromagnetic pulse in the rectangular waveguide with PEC lateral boundaries (figure 2). The waveguide is located along the x-axis and is of $W_y = \lambda/\sqrt{2}$ width and of $W_z = W_y/2$ height, where $\lambda = 2\pi c/\omega$ is the length of EM wave in free space at the exciting frequency ω. The electric field was excited at the tetrahedron edges of the the initial section using

$$E_x = E_y = 0, \qquad E_z = \begin{cases} 0 & t < 0 \\ \sin(\omega t - k_x x_0) & t > 0 \end{cases} \tag{14}$$

where $x_0(y,z)$ is the local x co-ordinate of the initial section, $k_x = \sqrt{\omega^2/c^2 - k_y^2 - k_z^2}$ is the x component of the wavevector $\boldsymbol{k} = \{k_x, k_y, k_z\}$. In our case only the TE^{+x}_{mn} mode is excited with $m = 1$ and $n = 0$ therefore $k_y = \pi m/W_y = \pi\sqrt{2}$, $k_z = \pi n/W_z = 0$ [5]. In the simulations $c = 1, \omega = 2\pi$ are taken hence $\lambda = 1, k_x = \pi\sqrt{2}$.

The mesh has 16 points per wave length in the free space. The length of the waveguide was taken to be 170λ which is large enough to avoid any reflection from the end of the waveguide. The mesh consists of 350085 points and 2100512 elements. Safety factor of 0.8 was used in this simulation.

Comparison between exact and numerical solution are presented in figure 5. Here the E_z component at the waveguide axis after 200 cycles is plotted. The region of transition from the forerunner to the main signal with currier frequency is shown. The currier frequency signal is propagating with the group velocity

$$C_g = \frac{d\omega}{dk_x} = \frac{c^2}{\omega}\sqrt{\frac{\omega^2}{c^2} - k_y^2 - k_z^2} \quad < c \tag{15}$$

For the case in hand $C_g = c/\sqrt{2}$ and the conventional boundary of the currier frequency signal arrival is indicated by the green dashed line in figure 5.

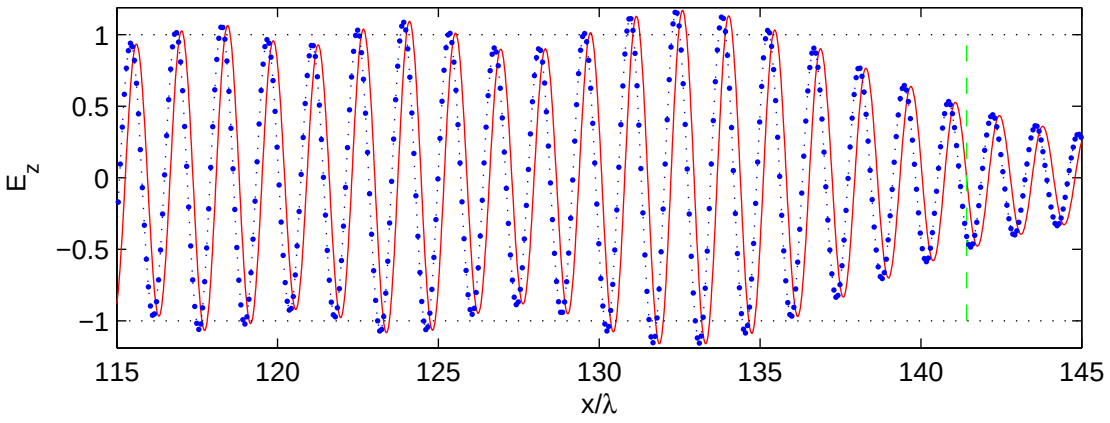

Figure 5: The E_z component at the waveguide axis exact (red) and numerical (blue) after 200 cycles. Green gashed line indicates $x = C_g t$.

It can be seen that despite the large distance, 140λ, propagated by the wave the local amplitude was perfectly resolved by the integration method. However, similar to the Yee scheme on structured grid a small phase shift can be observed.

4.2 Scattering on a polyhedra

In order to validate the scheme for the problem of scattering of EM waves by PEC body a polyhedron shape was considered.

A 12-faces PEC polyhedron with an electric length of 2λ, figure 6, was fitted into a 3D ideal mesh. The truncated far field was taken at 3 wavelength away from the scatterer to minimize the effect of any reflection from the outer boundaries.

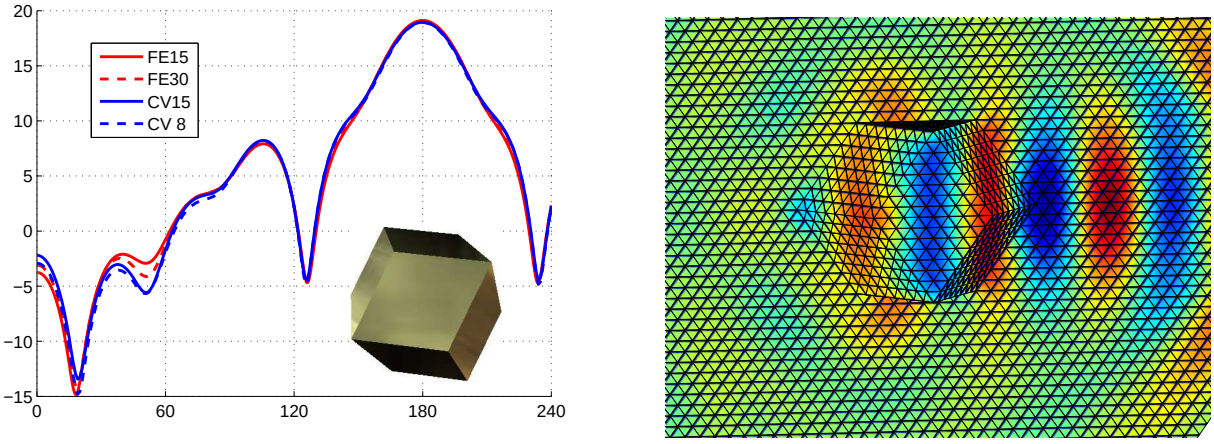

Figure 6: Radar Cross Section (RCS) in the vertical plane and polyhedron (left). Mesh and E_z component of the scattered field (right).

Figure 6 (left) shows the RCSs computed by the two step Galerkin Finite Elements method(red) and the generalized Yee method(blue). The results show that the local discrepancy in RCS obtained by the new scheme for meshes with 15 points per wavelength (solid) and 8 points per wavelength (dashed) is much less than that obtained by the FE method using meshes with 30 points per wavelength (dashed) and 15 points per wavelength(solid). The CPU time required, using the generalized Yee scheme, to compute the solution on the mesh with 15 points per wavelength and consists of 915584 points and 5349240 elements, was 1000 seconds on Pentium 4 PC. In comparison, the same mesh required 4000 seconds to compute the solution using the traditional finite elements methods.

4.3 Fully unstructured mesh

The final example involves the scattering of electromagnetic waves by a PEC sphere. The electical length of the sphere is taken to be 2λ. A spherical domain of a radius 8λ is chosen to enclose the PEC sphere. The mesh generated using the new proposed method is shown in figure 4. 15 points per wavelength were employed in the descritisation of the surface of the scatterer while 6 points per wavelength were used for the descritisation of the far field boundary. The mesh consists of 38748 points and 218816 elements.

The number of time-steps required for a complete cycle was 54. The CPU time required

to complete 3 cycles was 32 s. The computed Radar Cross Section (RCS) was plotted in figure 7 and compared to the analytical solution. It can be seen that very good accuracy was achieved using the generalized Yee scheme on this type of meshes.

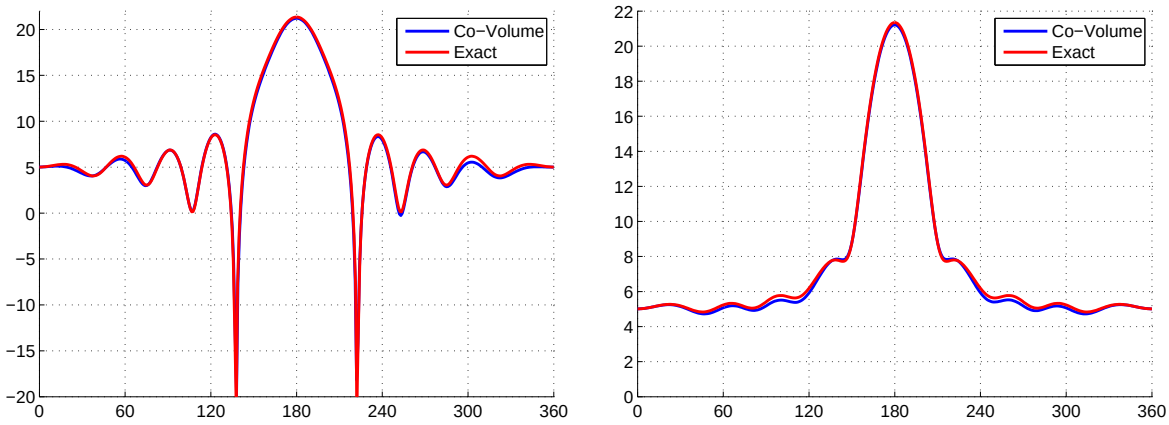

Figure 7: Radar Cross Section exact (red) and computed by the co-volume method (blue) in vertical plane (left) and horizontal plane (right).

5 CONCLUSIONS

The co-volume method for the integration of the Maxwell's equations has been implemented. To produce appropriate meshes for the proposed scheme, a new mesh generation methods based on combining a modified advancing front method for point placement and Delaunay triangulation for element generation was developed. The code has been tested on few different meshes. Simulation of EM wave propagation in a long waveguide shows that the scheme keeps perfectly the amplitude. Simulation of the scattering on 3D bodies shows that accuracy of co-volume method is superior to the standard Finite Element method if the body has sharp edges and singularity. The simulation also demonstrate high efficiency of the co-volume method.

REFERENCES

[1] K. Yee. Numerical solution of initial boundary value problem involving Maxwell's equation in isotropic media. *IEEE Trans. Antennas and Propagation.* **14**, 302–307, (1996)

[2] K. Morgan, O. Hassan O and J. Peraire. A time domain unstructured grid approach to the simulation of electromagnetic scattering in piecewise homogeneous media. *Computer Methods in Applied Mechanics and Engineering.* **134**, 17–36, (1996).

[3] A. Taflove and S.C. Hagness, *Computational Electrodynamics: The Finite–Difference Time Domain Method*, 2nd ed., Artech House, Boston, 2000.

[4] R.A. Nicoladies and Q.–Q. Wang, Convergence analysis of a co–volume scheme for Maxwell's equations in three dimensions, *Mathematics of Computation*, **67**:947–963, 1998.

[5] C.A. Balanis. *Advanced engineering electromagnetic*, Wiley, (1989).

[6] A. Taflove and M.E. Brodwin. Numerical solution of steady state electromagnetic scattering problems using the time dependent Maxwell's equation. *IEEE Trans. Microwave Theory Tech.* **23**, 623–630, (1975).

[7] D.J.Naylor. Filling space with tetrahedra. *International Journal for Numerical Methods in Engineering*. **44**, 1383–1395, (1999).

[8] I. Sazonov, D. Wang, O. Hassan , K. Morgan and N.P. Weatherill, A stitching method for the generation of unstructured meshes for use with co-volume solution techniques. *Computer Methods in Applied Mechanics and Engineering*. **195**, 1826–1845, (2006).

[9] P.L. George and H. Borounchaki, *Delaunay Triangulation and Meshing. Application to Finite Elements*, Hermès, Paris, (1998).

[10] Q. Du, V. Faber and M. Gunzburger. Centroidal Voronoi Tessellations: Applications and Algorithms. *SIAM Review*. **41**(4), 637–676, (1999).

[11] P.M. Knupp. Algebraic mesh quality metrics. *SIAM J. Sci. Comput.* **23**(1), 193–218, (2001).